

1 *Type of the Paper (Article, Review, Communication, etc.)*

2 **Impact of Plug-in Electric Vehicles Integrated into** 3 **Power Distribution System based on Voltage** 4 **Dependent Power Flow**

5 **Yuttana Kongjeen¹ and Krischonme Bhumkittipich^{1,*}**

6 ¹ Department of Electrical Engineering, Rajamangala University of Technology Thanyaburi,
7 Pathumtani, Thailand;

8 * Correspondence: krischonme.b@en.rmutt.ac.th; Tel.: +66-02-549-3571

9

10 **Abstract:** This paper proposes the impact of plug-in electric vehicles integrated into power
11 distribution system based on voltage dependent control. The plug-in electric vehicles was modeled
12 as the static load model in power distribution systems under balanced load condition. The power
13 flow analysis is determined by using the basic parameters of the electrical network. The main point
14 of this study are compare with voltage magnitude profiles, load voltage deviation, and total power
15 losses of the electrical power system. There are investigating the affected from constant power load,
16 constant current load, constant impedance load and plug-in electric vehicles load, respectively. The
17 IEEE 33 bus test system is used to test the proposed method by assigning each load type to a
18 balanced load in steady state and applied the solving methodology based on the bus injection to
19 branch injection matrix, branch current to bus voltage matrix, and current injection matrix to solve
20 the power flow problem. The simulation results showed that the plug-in electric vehicles load had
21 the lowest impact compared to other loads. The lowest plug-in values for the electric vehicle loads
22 were 0.062, 119.67 kW and 79.31 kVar for the load voltage deviation, total active power loss and total
23 reactive power loss, respectively. Therefore, this study can be verified that the plug-in electric
24 vehicles load were affected to the lowest of the electrical power system in condition to same sizing
25 and position. So that, in condition to the plug-in electric vehicles load added into the electrical power
26 system with the conventional load type or complex load type could be considered that the affected
27 from the plug-in electric vehicles load in next study.

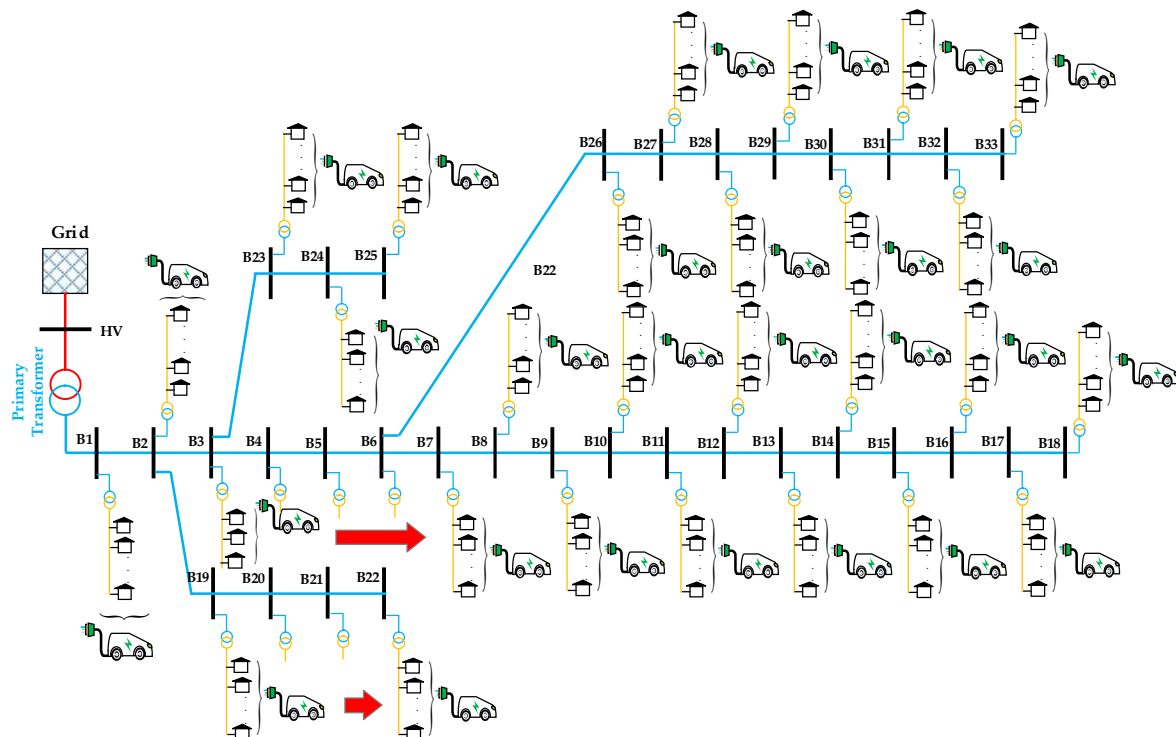
28 **Keywords:** load flow analysis; load voltage deviation; plug-in electric vehicles load; power-flow
29 analysis; static load models.

30

31 **1. Introduction**

32 The complexity of different load types has affected the advancement of power electronic
33 technology and devices in daily life. There are also studies on the features of modern loads to solve
34 problems in the electrical system. The plug-in electric vehicles (PEVs) are a growing burden in the area
35 of power systems. The use of PEVs is likely to increase. It can reduce the emission of carbon dioxide
36 that is harmful to the environment and affects the global warming. Including the public sector,
37 promotion and privileges such as taxation or privilege in special areas. The advantage of PEVs arises
38 from its use of fuel cells as well as battery energy storage, and it converts and combines power to
39 traction drive systems. The electrical power system was connected with an electric wiring cable to the
40 AC-DC power converters that called the battery charger used for charging the battery packs of PEVs
41 when a low level state of charge (SOC). Generally, the PEVs is defined in slow charging mode for
42 consuming the energy from the electrical power system [1]. As Figure 1 shows, the high penetration

43 of PEVs connected to the each household and consumed energy from the grid. Interestingly, in
 44 condition to recharge of the battery for instantaneous time on same time of the every PEVs may be
 45 more effected to the electrical power system.
 46



47
 48
 49

Figure 1. PEVs connected in the radial distribution system

50

51 Meanwhile, the impact of electric vehicles on fast charging is to reduce system voltage stability.
 52 Charging of the battery depends on the charging type of the EVs battery installed in each charging
 53 station^[2]. Energy sources are needed to support the expansion and power requirements of electrical
 54 equipment in the installed system. Generally, the energy source comes from the conventional source
 55 of energy and combine with renewable energy. Therefore, the risk assessment of the electrical system
 56 of the distribution system. By analyzing the charging behavior of electric vehicles during charging
 57 and convert the power of the electric vehicle into the electrical system randomly. It can prevent and
 58 reduce the risk of controlling on the power distribution system^[3]. Electric vehicle batteries (BEVs) and
 59 electric vehicle loads (EVs) have been presented by considering the effect on V2G and G2V power
 60 curves; In terms of power demand from the electrical system. The level of penetration of BEVs and
 61 EVs at different levels of the electrical power system. The effect of these loads on the electrical system
 62 was presented in ^[4]. The uncertainly propagate of charging from PEVs load were effected to reduce
 63 aging of transformer in condition to loss increase, insulation lift, the hot spot temperature which is
 64 using daily load profiles to simulate the impact of PEVs. Meanwhile, the effect from unbalance load
 65 not considered ^[5]. Therefore, Smart charging need to manage for increasing long lift time of the
 66 transformer ^[6] and improved suitable condition for energizing of transformer by using smart
 67 transformer type ^[7]. The one type of methodology from smart charging is coordinated charging of
 68 PHEVs that can be reduced distribution system losses ^[8]. The objective function from triangle
 69 equivalence of losses, load factor and load variance are used to find the optimal condition on PHEVs
 70 demand load profiles ^[9]. Furthermore, in the electrical power system networks are connecting
 71 thought transmission lines. Therefore, distribution feeder reconfiguration can be adapted for
 72 managing the energy consumption from the PHEVs that method can reducing expected cost and total
 73 power loss reduction from variance of penetration level of PEVs in the electrical power system ^[10].

74 Additionally, the user benefits are become key issue to manage in term of reduce the cost of battery
75 capacity degradation, electricity cost and waiting time for charging battery. So that, the charging
76 management should be controlled in optimal scheduling and pay back the most benefits to EV car
77 owners/11). The aggregated EV charging demand need to determine and investigate in term of
78 uncertain any pattern of EV load in the electrical power system, which are relevant an agent based
79 approach. The agent-based approach consists EV type, battery and charging process, charging
80 infrastructure, mobility and social, respectively. Monte Carlo techniques were used to define charging
81 demand and charging scenarios, which are revealed voltage profiles reduced during on peak demand
82 charging and should be controlled in condition balance and unbalance load/12-14). The reliability
83 evaluation of a distribution network by combined with distribution generator(DG), battery
84 storage(BS) and electric vehicles(EVs) revealed EVs in discharging mode or V2G technology can be
85 supply the power to grids and the EVs should be controlled in limits on recharging mode for
86 increasing high reliability from the evaluation/15). Consequently, the PEVs can be reduced the impact
87 from charging mode in same time or in same power transmission line by using the V2G technology
88 and combined with smart grids control /1, 16-21). The smart grids control concept are need to manage
89 in optimal condition all relevance; such as power sources, transmission system, distribution system,
90 user benefits and economics /22-24). Therefore, optimization techniques are applying to find the
91 optimal solution any problems that effected from PEVs increasing and high consume the energy
92 power from the electrical power system networks /11, 25-27).

93 In power flow studies, the generally practice is to present the composite load characteristics at
94 the point common coupling of electrical power system. The load models consist of static load models
95 and dynamic load models, which the static load model is selected for the proposed study. The static
96 load models consists of voltage dependency and frequency dependency of the load characteristics
97 /28-30). The purposed of paper considered the voltage dependency of load characteristics by using the
98 exponential model to solve the difference type of load models. The battery charger in normal mode
99 charging or slow charging was represented the characteristics of PEVs, which described in an
100 exponential load by testing in the laboratory /31). Many researchers were studied and showed from
101 proposed in impact from PEVs for the electrical power system network as in above, but not
102 considerate in the actual behavior of the PEVs under voltage dependent power flow. So that, this
103 study is interesting to investigate the PEVs load model based on exponential load characteristics by
104 considering in the static load. With numerical investigations, the voltage dependent power flow is
105 used to solve by comparison with the conventional load type (Z, I, P) found in the IEEE 33 bus radial
106 distribution test system. This means that is also defined in a balanced load system to find the total
107 power losses and the load voltage deviation of the electrical power system.

108 The structure of the paper is as follows: the load flow study (LF) for power flow analysis is
109 presented in Section 2, and the proposed conventional load (Z, I, P), PEVs based on static load models
110 is presented in Section3. Section 4, presents the total power losses in the electrical power system. The
111 test radial distribution system is provided in Section5. Section6 proposes the simulation results and
112 explanation. Finally, the conclusion and discussion are given in Section 7.

113

114 2 Proposed Load Flow Study and Formulation

115 The Load flow study (LF) is very important in the planning of modern power system or in
116 condition to improve the existing system, to considerate the some issues that may be effect to
117 planning design part, operation part and control part. The key point of LF the power system network
118 is using to solve the steady state solution which are provides the information on voltage magnitude
119 and phase angle, active power reactive power flow and total power loss, respectively. To understand
120 the impacts of PEVs on LV networks considering the amount of PEVs and behavioral uncertainties,
121 a static framework is proposed which can be applied to any type of conventional loads of the electrical
122 load system and PEVs load. In order to investigate the impact of PEVs load effected on the electrical

123 power system under slow charging mode of the battery charger. The solving methodology is using
 124 relevant based on three delivered metrics, the bus injection to branch injection matrix (BIBC), branch
 125 current to bus voltage matrix (BCBV) and current injection matrix (I), respectively. In this section, will
 126 be applying the PEVs load and analyzed the effected into the electrical power system as follows.
 127 The BIBC, BCBV and I are simplify to analyze the radial distribution network (RDN) and can be adapt
 128 the PEVs load into algorithm [32]. Basically, the component of complex power load (S_k) and injection
 129 current (I_k^t) on the bus k can be showing as (1) and (2), respectively.

$$S_k = P_k + jQ_k \quad k = 1 \dots N \quad (1)$$

130 Where N is total number of bus in the radial distribution network. P_k and Q_k are active power
 131 and reactive power of load at bus k .

132 Therefore, can be rearranged the equivalent injection current at the t iteration of solution from
 133 any bus to I matrix is.

$$I_k^t = I_k^r (V_k^t) + jI_k^i (V_k^t) = \left(\frac{P_k + jQ_k}{V_k^t} \right)^* \quad (2)$$

134 Where V_k^t are bus voltage and I_k^t equivalent injection current, respectively. Meanwhile, the
 135 equivalent injection current consists of real part (I_k^r) and imaginary part (I_k^i). Both of bus voltage and
 136 equivalent injection current are considerate at the t iteration of solution.

137

138 Kirchhoff's Current Law (KCL) is applied to solve the power flow of RDN from relationship
 139 between bus current injections and branch currents by formulating the branch currents from current
 140 any branch to the equivalent current injections can be showed as

$$[\mathbf{B}] = [\mathbf{BIBC}][\mathbf{I}] \quad (3)$$

141 Where \mathbf{I} is represented the current injection matrix, \mathbf{BIBC} is represented the branch injection to
 142 branch current matrix and \mathbf{B} represented the current each branches, respectively. Generally, the
 143 \mathbf{BIBC} was obtained number 1 or 0 only and upper triangular matrix.

144

145 Meanwhile, relationship between branch currents to bus voltages can be showing a function of
 146 branch current, line parameters and the substation voltages as

$$[\Delta \mathbf{V}] = [\mathbf{BCBV}][\mathbf{B}] \quad (4)$$

147 Where \mathbf{BCBV} is represented the branch currents to bus voltages matrix and $\Delta \mathbf{V}$ represented the
 148 voltage difference from root node to each branch current.

149

150 The \mathbf{BCBV} and \mathbf{BIBC} are combined with relation between current injections and bus voltages
 151 of the RDN can be expressed as.

$$\left. \begin{aligned} [\Delta \mathbf{V}] &= [\mathbf{BCBV}][\mathbf{BIBC}][\mathbf{I}] \\ &= [\mathbf{DLF}][\mathbf{I}] \end{aligned} \right\} \quad (5)$$

152 So that, voltage solution of the RDN each t iteration can be expressed as

$$[\Delta \mathbf{V}^{t+1}] = [\mathbf{DLF}][\mathbf{I}^t] \quad (6)$$

153

154 **3. Static Load Models and Load Voltage Deviation**

155 3.1 Static load model

156 A load model of the electrical power system is defined by expressing the character instantaneous
 157 of time and then represented as an algebraic function based on the frequency or the bus voltage
 158 magnitude at that instant Basically, the apparent load power (kVA) can be considered separately to
 159 the active power component and the reactive power component, respectively. Generally, the voltage
 160 dependent of the load behavior at each bus is represented by the exponential model as [28].

$$P_{Lk} = P_{Lk0} \left(\frac{V_k}{V_{ko}} \right)^{n_{pi}} \quad (7)$$

$$Q_{Lk} = Q_{Lk0} \left(\frac{V_k}{V_{ko}} \right)^{n_{qi}} \quad (8)$$

$$S_{Lk} = P_{Lk} + jQ_{Lk} \quad (9)$$

161 where n indicates amount of the PQ bus in the electrical power system, S_{Lk} , P_{Lk} and Q_{Lk} indicates
 162 represented the nominal apparent power, active power and reactive power, respectively. Meanwhile,
 163 V_{i0} is represented the magnitude of the bus nominal voltage, n_{pi} and n_{qi} are represented the load
 164 indices from each load type.

165 The PEVs is a hybrid automobile by combining with the combustion engine and the electric
 166 motor for traction drive. Meanwhile, energy source to feed the electric motor control with battery that
 167 can be recharged by connecting to the electrical network Therefore, the PEVs in the electrical network
 168 was represented by using the battery charger which is also to convert the AC-DC converter for
 169 charging the battery. In order to considerate in slow charging mode of charger can be represented the
 170 character instant of time as an algebraic function by using the exponential model, as in [31]. So that,
 171 from (10) and (11) is concerned the load power factor value of the battery charger, which considerate
 172 when installed.

$$P_{PEVs} = S_0 \times kp \times \left(\frac{V_i}{V_{i0}} \right)^{n_{pi}} \quad (10)$$

$$Q_{PEVs} = S_0 \times kq \times \left(\frac{V_i}{V_{i0}} \right)^{n_{qi}} \quad (11)$$

$$S_{PEVs} = P_{PEV} - jQ_{PEV} \quad (12)$$

173 where S_0 indicates the apparent load power (kVA) at nominal voltage V_{i0} , kp is represented the
 174 load power factor pf and can be found $k_q = \sqrt{(1 - pf^2)}$.

175

176

Table 1. Exponential indices value of load type

Load Type	n_{pi}	n_{qi}
Constant impedance (Z)	2	2
Constant current (I)	1	1
Constant power (P)	0	0
PEVs/31j	2.59	4.06

177

178 Table 1, shows the constant indices of load types used to solve the power flow problem on the
 179 electrical power system. The indices consist of a constant impedance load, constant current load,
 180 constant impedance load and PEVs, respectively. The PEVs are specified on the slow charging model
 181 of the battery charger used in this study.

182

183 3.2. Load Voltage Deviation (LVD)

184 The increasing load on the power system will affect the voltage level in each bus. Therefore, the
 185 LVD is used to analyze the deviation of the bus voltage that is affected by the load. In general, the
 186 LVD value must be minimal. It shows that the system still has a good level of voltage. Therefore, the
 187 change in load on each bus must be appropriate, as described in (13), (33-34).

$$LVD = \sum_k^n \left(\frac{V_k^{ref} - V_k}{V_k^{ref}} \right)^2 \quad (13)$$

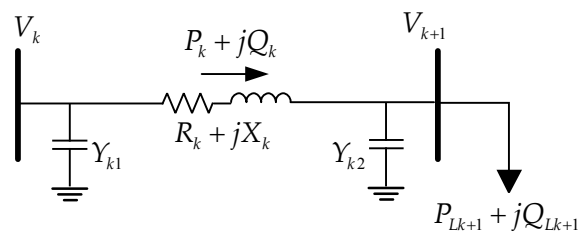
188 where V_k is represented bus load voltage of each load. Meanwhile, V_k^{ref} is represented voltage
 189 reference under normal conditions that is also defined at 1 p.u.

190

191 4. Total Power Loss of Electrical Power System

192 Generally, all electric appliance or loads of the electrical power system will be variance from
 193 behavioral of the loads characteristic. Therefore, the total real and reactive power loss in the system
 194 used to evaluate in the level of impact when loads increasing in the electrical power system can be
 195 calculated using (19) and (20) as follows (35).

196



197

198

199

200

Figure 2 Electrical equivalent circuit of a typical branch k

$$P_{k+1} = P_k - P_{Loss,k} - P_{Lk+1} \quad (14)$$

$$= P_k - \frac{R_k}{|V_k|^2} \left\{ P_k^2 + \left(Q_k + Y_k |V_k|^2 \right)^2 \right\} - P_{Lk+1} \quad (15)$$

$$Q_{k+1} = Q_k - Q_{Loss,k} - Q_{Lk+1} \quad (16)$$

$$= Q_k - \frac{X_k}{|V_k|^2} \left\{ P_k^2 + \left(Q_k + Y_k |V_k|^2 \right)^2 \right\} - Y_{k1} |V_k|^2 - Y_{k2} |V_{k+1}|^2 - Q_{Lk+1} \quad (17)$$

$$|V_{k+1}|^2 = |V_k|^2 + \frac{R_k^2 + X_k^2}{|V_k|^2} (P_k^2 + Q_k^2) - 2(R_k P_k + X_k Q_k) \quad (18)$$

$$= |V_k|^2 + \frac{R_k^2 + X_k^2}{|V_k|^2} \left(P_k^2 + \left(Q_k + Y_k |V_k|^2 \right)^2 \right) - 2 \left(R_k P_k + X_k \left(Q_k + Y_k |V_k|^2 \right) \right) \quad (19)$$

201 The active and reactive power in the transmission line section are connecting buses k and $k + 1$
 202 can be calculating as

$$P_{Loss}(k, k + 1) = R_k \cdot \frac{(P_k^2 + Q_k^2)}{|V_k|^2} \quad (20)$$

$$Q_{Loss}(k, k + 1) = X_k \cdot \frac{(P_k^2 + Q_k^2)}{|V_k|^2} \quad (21)$$

203 The power loss from a transmission line consists of active and reactive. Therefore, the total active
 204 power loss ($P_{T,loss}$) and the total reactive power loss ($Q_{T,loss}$) of the electrical power system are
 205 using summarize the losses of all transmission line in the system, which are given as

$$P_{T,Loss} = \sum_{k=1}^n P_{Loss}(k, k + 1) \quad (22)$$

$$Q_{T,Loss} = \sum_{k=1}^n Q_{Loss}(k, k + 1) \quad (23)$$

206 Using this efficient voltage dependent power flow technique, the total losses and voltage at
 207 each bus of the electrical power system were assessed.

208 5. Radial Distribution System(RDS) for testing from purpose

209 The propose in this study selects a primary distribution system to evaluate the impact of each
 210 load type on the power system network. The IEEE 33 bus test system has been used to obtain results
 211 and to evaluate the efficiency of each type of load test. By determining base MVA = 100, base voltage
 212 = 11 kV. Generally, the IEEE 33 bus test system is defined by consisting of 32 line sections with a total
 213 power constant load of 3.72 MW and 2.3 MVar in the balanced load system shown as in [36]. Generally,
 214 the RDS was interested and used to solve many problem from the system for proving and comparing
 215 each based case. Therefore, this paper was considered the IEEE33 bus test system for solving the
 216 impact of PEVs integrated into power distribution system based on voltage dependent power flow.
 217 The IEEE33 bus test system was modified the traditionally load models to voltage dependent load
 218 models. The LF methodology was applied to analyze and compare each load type by using voltage
 219 profiles, total power loss and LVD. This paper was supposed in condition of balance load for any
 220 load to install each bus of the power system and trying change load type by changing the exponential
 221 indices for each loads by using data in Table 1.

222

223 6. Simulation Results

224 The proposed each load type and LF algorithm were implemented in a MATLAB m-file. The LF
 225 was solved based on the balance load of constant impedance load (Z), constant current load (I),
 226 constant power load (P) and PEVs obtained using the static analysis of the electrical power system.
 227 In this paper, we assume that each type of load installed in the electrical system is the same load for
 228 each cycle analysis and the load type change is complete. Therefore, the number of conventional load
 229 (Z, I, P) and PEVs will distribute each at the RDS buses. The results show the bus voltage, total power
 230 loss and LVD for each type of load, as given in Table 2, Figure 3, Table 3, Figure 4 and Table 4,
 231 respectively.

232 The basic steps of load flow analysis for RDS are as follows.

- 233 Step 1: Read data for using in calculation, which consists of buses data, lines data and exponential
 234 indices value of load type.
- 235 Step 2: Initial voltage profiles (V_0) and (V_k) for all bus at $1\angle 0^\circ$.
- 236 Step 3: Form the BIBC matrix by using data in step 1.
- 237 Step 4: Form the BCBV matrix by using data in step 1.
- 238 Step 5: Form the DLF matrix by using data in step 1.
- 239 Step 6: Set the exponential indices of each load types j
- 240 $j=1$ (Z load; P=2 and Q=2)
- 241 $j=2$ (I load; P=1 and Q=1)
- 242 $j=3$ (P load; P=0 and Q=0)
- 243 $j=4$ (PEVs; P=2.59 and Q=4.06)
- 244 Step 7: Define iteration count $t = 0$ and tolerance convergence (ε) = 0.0001.
- 245 Step 8: Iteration $t = t + 1$.
- 246 Step 9: Compute the equivalent current injection (I_k^t) from (2) based on individual type of each load
 247 on (7)-(12) for finding complex power (S_k^t) and using the exponential indices from Table 1, for
 248 applying voltage dependent power flow.
- 249 Step 10: Calculate the bus voltage using Equation (6) as $[\Delta \mathbf{V}^{t+1}] = [\mathbf{DLF}][\mathbf{I}^t]$.
- 250 Step 11: Check the mismatches. If $\max(\text{abs}(V_{new} - V_{old})) \leq \varepsilon$, go to Step 8 else go to step 12
- 251 Step 12: Calculate the final voltage at each bus, LVD and the total power loss from (13), (22), and (23).
- 252 Step 13: Print the bus voltage magnitude, LVD and total power loss
- 253 Step 14: $j = j + 1$
- 254 Step 15: Check the exponential indices. If $j \leq 4$, go to Step 7, else go to step 16.
- 255 Step 16: Stop
- 256
- 257

Table 2 Comparison voltage profiles of IEEE 33 bus test system load-flow results

Bus No.	Z(p.u.)	I(p.u.)	P(p.u.)	PEVs(p.u.)
1	1.0000	1.0000	1.0000	1.0000
2	0.9973	0.9972	0.9970	0.9977
3	0.9847	0.9839	0.9829	0.9873
4	0.9782	0.9769	0.9755	0.9820
5	0.9717	0.9701	0.9681	0.9768
6	0.9558	0.9530	0.9497	0.9631
7	0.9527	0.9498	0.9462	0.9602
8	0.9485	0.9453	0.9413	0.9572
9	0.9432	0.9395	0.9351	0.9532
10	0.9382	0.9342	0.9292	0.9494
11	0.9374	0.9334	0.9284	0.9489
12	0.9362	0.9320	0.9269	0.9480
13	0.9310	0.9264	0.9208	0.9441
14	0.9290	0.9243	0.9185	0.9426
15	0.9278	0.9230	0.9171	0.9418
16	0.9267	0.9218	0.9157	0.9410
17	0.9250	0.9199	0.9137	0.9396
18	0.9245	0.9194	0.9131	0.9392
19	0.9968	0.9967	0.9965	0.9972
20	0.9933	0.9931	0.9929	0.9939

21	0.9926	0.9924	0.9922	0.9932
22	0.9919	0.9918	0.9916	0.9926
23	0.9813	0.9804	0.9794	0.9843
24	0.9750	0.9739	0.9727	0.9788
25	0.9719	0.9707	0.9694	0.9760
26	0.9541	0.9512	0.9477	0.9617
27	0.9519	0.9489	0.9452	0.9598
28	0.9421	0.9383	0.9337	0.9507
29	0.9350	0.9308	0.9255	0.9441
30	0.9320	0.9275	0.9220	0.9414
31	0.9285	0.9237	0.9178	0.9385
32	0.9277	0.9229	0.9169	0.9378
33	0.9274	0.9226	0.9166	0.9376

258

259

260

261

262

263

264

265

266

267

268

269

270

In Table 2, it is possible to see the voltage magnitude profiles by arranging from bus No.1 to bus No.33 under difference load types and voltage level are reduce from the root node to the end of node. Therefore, the effect of load and transmission line are reducing level of the voltage profile and increasing the total power loss. The results are the voltage magnitude profiles by using the voltage dependent power flow to solve the effect from difference load types. The simulation results show the lowest voltage each load types on bus No.18 (the bold text number). There are arrange from high to low of the voltage profiles; 0.9392 p.u., 0.9245 p.u., 0.9194 p.u. and 0.9131 p.u., by represented PEVs load, Z load, I load and P load, respectively. Therefore, in this case the weak point found that effected from power constant by comparing but same as tending point from contour static voltage magnitude profiles each load types in the weak point. Additionally, the simulation results are show in a static power analysis by using on average peak value of power demand from each load and enough for representing the characteristic to the RDN.

271

272

273

274

275

276

277

278

279

280

281

Figure 3 shown the contour of static voltage magnitude profiles are comparing with Z load, I load, P load and PEVs, respectively. The graphic show the lowest contour voltages profiles remain about 0.9130 p.u. (red color field) and the highest contour voltages profiles remain about 1 p.u. (violets color field). Interestingly, the static voltage analysis by applying contour color can show some details of the characteristic from each any load. Especially, the PEVs load of the contour of static voltage magnitude profiles are reveal that affect in the lowest level in the RDN when compared with any load types. In order to arrange the level from the highest to the lowest impact of the RDN are constant power load, constant current load, constant impedance load and PEVs, respectively. Therefore, the Z load, I load, P load and PEVs affected by considering to static voltage stability based on the voltage profiles obtained from the electrical power system. In decreasing order, the factors that affect the static voltage stability were P load, I load, Z load, and PEVs, respectively.

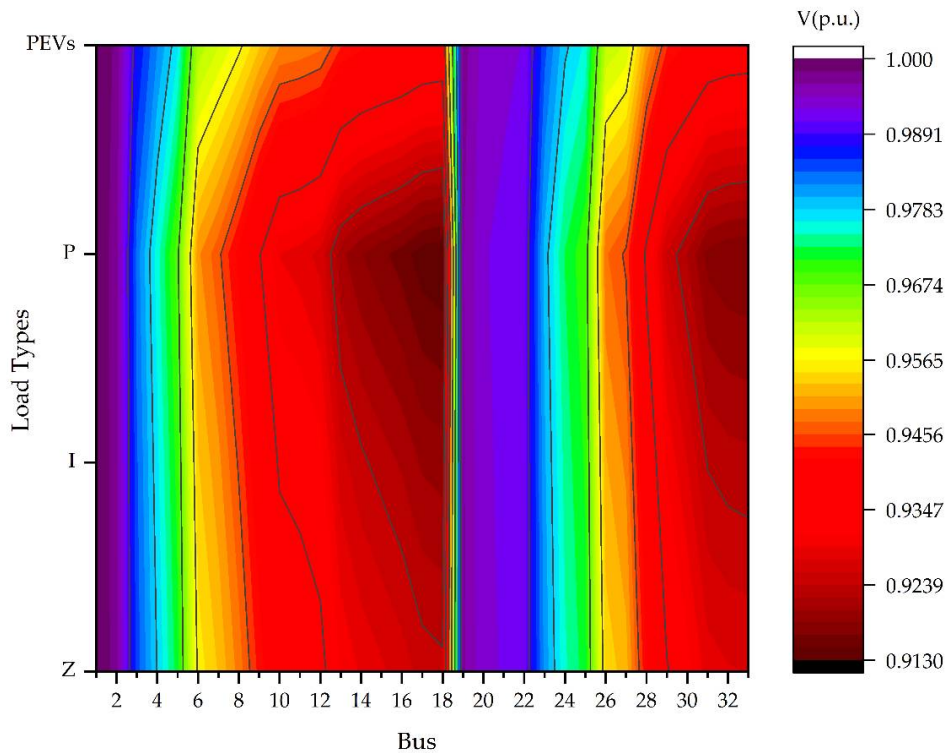


Figure 3. Contour of static voltage profiles from difference load type

282

283

284

285 Table 3, demonstrate that all effects from each load model types to the transmission line losses
 286 from transmission line No.1 to transmission line No.32. The total power losses are derive from the
 287 current flow thought a transmission line between two buses that affected from load are installed on
 288 any the buses. The sizing and location of the transmission line loss were effected to voltage drop in
 289 the power system and in condition to install near the root node that should be carry burden from
 290 current thought to the end of node. However, in the realistic many factor and details to effect the loss
 291 from cable such as temperature, installation method, type of cable etc, The simulation results from
 292 Table 3, showed in condition to transmission line loss in Kilowatt unit(kW) of each transmission line
 293 in the RDN. In this case, the transmission line No.2 was effected more transmission line loading than
 294 another of each transmission line. In this case compare with each load types from the highest to the
 295 lowest(the bold text number) are 51.791 kW, 45.975 kW, 41.469 kW, and 30.940 kW which rearrange
 296 load types from P load, I load, Z load and PEVs, respectively. In condition, if compare on the second
 297 order from the highest to the lowest found that (the italic text number) on the transmission line
 298 number No.5 are 38.249 kW, kW, kW, and kW, that derived same as, from P load, I load, Z load and
 299 PEVs, respectively. So that, the total power loss in the transmission lines can reducing and improving
 300 from this weak point but that out of scope in this work.

301

302

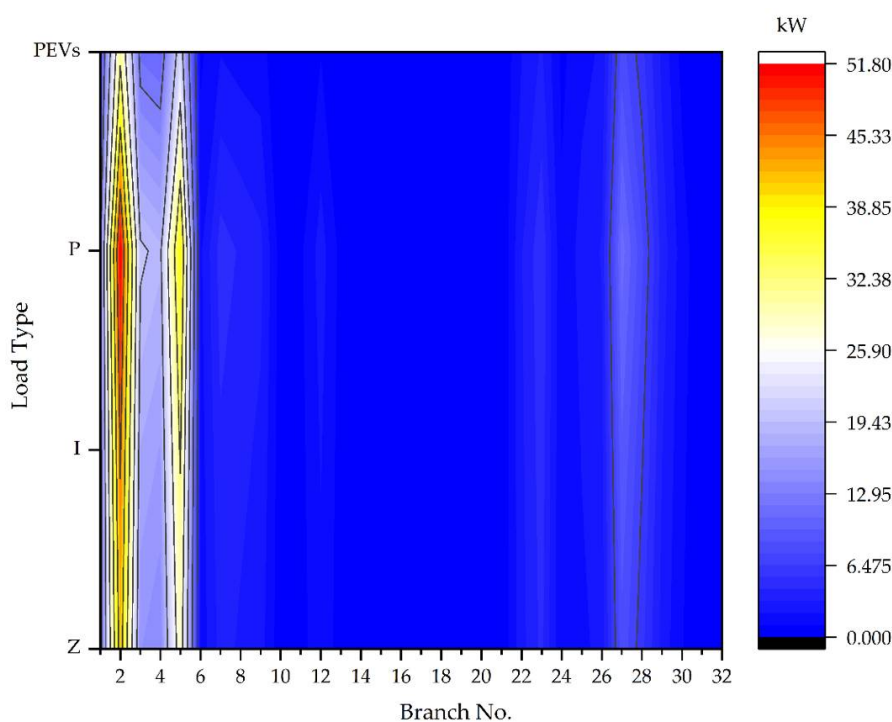
Table 3. Comparison of IEEE 33 bus test system from lines active power loss results

Br.	No	Z(kW)	I(kW)	P(kW)	PEVs(kW)
	1	10.031	10.999	12.240	7.613
	2	41.469	45.975	51.791	30.940
	3	15.190	17.217	19.900	11.499
	4	14.134	16.095	18.699	10.615
	5	<i>28.793</i>	<i>32.849</i>	<i>38.249</i>	<i>21.652</i>
	6	1.457	1.654	1.915	0.868
	7	3.625	4.145	4.838	2.094
	8	3.075	3.546	4.181	1.693

9	2.606	3.012	3.561	1.471
10	0.404	0.467	0.554	0.235
11	0.640	0.742	0.881	0.359
12	1.927	2.240	2.666	1.033
13	0.526	0.612	0.729	0.265
14	0.256	0.299	0.357	0.094
15	0.201	0.235	0.281	0.091
16	0.179	0.210	0.252	0.086
17	0.038	0.044	0.053	0.021
18	0.157	0.159	0.161	0.140
19	0.807	0.819	0.832	0.707
20	0.098	0.099	0.101	0.085
21	0.042	0.043	0.044	0.037
22	2.852	3.005	3.182	2.144
23	4.596	4.850	5.144	3.402
24	1.143	1.210	1.287	0.835
25	1.931	2.217	2.601	1.789
26	2.460	2.831	3.329	2.328
27	8.315	9.588	11.301	8.052
28	5.751	6.638	7.833	5.746
29	2.853	3.297	3.896	2.955
30	1.154	1.341	1.594	0.711
31	0.154	0.179	0.213	0.098
32	0.010	0.011	0.013	0.008

303

304



305

306

Figure 4 Contour of lines active power losses when difference load type

307

308

309

310

The results from Figure 4, were compared with the contour of lines active power loss magnitude profiles obtained for each load type in the IEEE 33 bus test system. All the simulation results shown the effect of the different lines active power loss profiles from the each load type. The Figure 4, shows

311 that the highest active power loss each the load type of red color contour at the transmission line
 312 number No.2., and the second order of highest active power loss each the load type on yellow color
 313 contour in the transmission line number No.5., respectively. The simulation results from the contour
 314 of line active power losses when difference load type are reveal the weak point of highest active
 315 power loss on the transmission lines. Meanwhile, the rest of all the transmission line showed in same
 316 as the contour color and in for the future need to analyze in deep details on line loading factor each
 317 transmission line.

318 From the resulting above, it can be observed that those all voltage profiles and all transmission
 319 line loss are vary from the exponential indices of load each types by using voltage dependent load
 320 power flow from purposed. Therefore, optimal model of load type clouded be selected and defined
 321 nearly about the behavioral of each load.

322

323 **Table 4.** Comparison of LVD, Total active power loss, and total reactive power loss.

Load Type	LVD	Active power loss (kW)	Reactive power loss (kVar)	Apparent Power Loss(KVA)	%LVD	%P	%Q
PEVs	0.062	119.67	79.31	143.56	-40.96%	-41.31%	-41.07%
Z	0.089	156.87	104.18	188.31	-22.60%	-22.91%	-22.70%
I	0.101	176.63	117.51	212.15	-12.85%	-13.04%	-12.91%
P/35, 37 _l	0.117	202.68	135.14	243.60	0.00%	0.00%	0.00%

324

325 Table 4, shows results of LF algorithm based on voltage dependent power flow by comparing
 326 the values of the total real power loss (P_{loss}), the total reactive power loss (Q_{loss}) and LVD, that values
 327 are different from the each load type. The total active power loss and the total reactive power loss of
 328 the PEVs shown are less than those of the Z, I, and P load. Meanwhile, it was the same as the LVD.
 329 Additionally, in condition to compare with the percentage by using based on the power constant load
 330 that revealed the variance of the PEVs more affected than Z, I, and P load. Interestingly, the PEVs
 331 show that it is not significantly by the voltage-magnitude profile and total power loss of the electrical
 332 power system. Generally, PEVs connected with another load into the network and should be
 333 considered at this point when large-scale of PEVs penetration and the conventional load of the power
 334 network combined. It is majorly impact of the electrical power system.

335 It is important to highlight that the effected to the LVD, total active power, and total reactive power
 336 are dependent on the type of load model installed in the RDS. Furthermore, the PEVs model are affect
 337 less than the Z, I, P load, in order to compare with one by one. Therefore, the PEVs may be effected
 338 to the electrical power system when plugs into the power system network thought the outlets by
 339 combining with the traditional load and high penetration of PEVs cloud be noted.

340

341 **7. Conclusion**

342 The proposed a simple algorithm with LF methodology has been applied using the m-files,
 343 MATLAB program environment for the IEEE33 bus test system simulation. In addition, the each load
 344 models are also defined to solve the problem by using on a balanced load in a radial distribution
 345 system (RDS). Different simulations have been performed on the each load models. There are consist
 346 a constant power load, constant current load, constant impedance load and PEVs, respectively. The
 347 simulation of each load on peak load value have been discussed with the RDS in detail. Therefore,
 348 the simulation results shown impact of each load type to the RDS and compared with the bus system
 349 which are total power loss and LVD. Among the results for the four proposed load models, the
 350 differences in the exponential indices value of load type reflect the behavior of each load on the
 351 voltage dependent power flow. Consequently, the PEVs from the simulation results showed the

352 affected to the RDS by less than a constant power load, constant current load, constant impedance
353 load. The PEVs in the test case revealed the lowest LVD and lowest total power loss values of 0.062,
354 119.67 kW and 79.31 kVar, respectively. Although, in daily life, the PEVs will be included or combined
355 to another load in peak or off peak demand, its same charging time or same power transmission line
356 of the electrical system and while simultaneously being charged. So that, large-scale of PEVs
357 penetration will be affected to the electrical power system and could be managed in the optimal
358 condition. Furthermore, proper management of PEVs in the each area of the battery charger can be
359 beneficial of the reduced impact to the electrical power system. Moreover, it can also be implemented
360 in other condition with PEVs charging clustered by coordinating the each charger with power grid
361 for increasing the static voltage stability of the electrical power system.

362

363 References

364

- 365 1 M. Yilmaz and P. T. Krein, "Review of the Impact of Vehicle-to-Grid Technologies on Distribution
366 Systems and Utility Interfaces," *IEEE Transactions on Power Electronics*, vol. 28, no. 12, pp. 5673-5689,
367 2013, DOI: 10.1109/TPEL.2012.2227500.
- 368 2 C. H. Dharmakeerthi, N. Mithulananthan, and T. K. Saha, "Impact of electric vehicle fast charging on
369 power system voltage stability," *International Journal of Electrical Power & Energy Systems*, vol. 57, pp. 241-
370 249, 2014/05/01/ 2014, DOI: 10.1016/j.ijepes.2013.12.005.
- 371 3 J. Yang, W. Hao, L. Chen, J. Chen, J. Jin, and F. Wang, "Risk Assessment of Distribution Networks
372 Considering the Charging-Discharging Behaviors of Electric Vehicles," *Energies*, vol. 9, no. 7, pp. 560-580,
373 2016, DOI: 10.3390/en9070560
- 374 4 M. Aziz, T. Oda, T. Mitani, Y. Watanabe, and T. Kashiwagi, "Utilization of Electric Vehicles and Their
375 Used Batteries for Peak-Load Shifting," *Energies*, vol. 8, no. 5, pp. 3720-3738, 2015, DOI: 10.3390/en8053720
- 376 5 H. Turker, S. Bacha, D. Chatroux, and A. Hably, "Low-Voltage Transformer Loss-of-Life Assessments for
377 a High Penetration of Plug-In Hybrid Electric Vehicles (PHEVs)," *IEEE Transactions on Power Delivery*,
378 vol. 27, no. 3, pp. 1323-1331, 2012, DOI: 10.1109/TPWRD.2012.2193423.
- 379 6 A. D. Hilshey, P. D. H. Hines, P. Rezaei, and J. R. Dowds, "Estimating the Impact of Electric Vehicle Smart
380 Charging on Distribution Transformer Aging," *IEEE Transactions on Smart Grid*, vol. 4, no. 2, pp. 905-913,
381 2013, DOI: 10.1109/TSG.2012.2217385.
- 382 7 M. Liserre, G. Buticchi, M. Andresen, G. D. Carne, L. F. Costa, and Z. X. Zou, "The Smart Transformer:
383 Impact on the Electric Grid and Technology Challenges," *IEEE Industrial Electronics Magazine*, vol. 10, no.
384 2, pp. 46-58, 2016, DOI: 10.1109/MIE.2016.2551418.
- 385 8 C. Cao, L. Wang, and B. Chen, "Mitigation of the Impact of High Plug-in Electric Vehicle Penetration on
386 Residential Distribution Grid Using Smart Charging Strategies," *Energies*, vol. 9, no. 12, pp. 1024-1049,
387 2016, DOI: 10.3390/en9121024.
- 388 9 E. Sortomme, M. M. Hindi, S. D. J. MacPherson, and S. S. Venkata, "Coordinated Charging of Plug-In
389 Hybrid Electric Vehicles to Minimize Distribution System Losses," *IEEE Transactions on Smart Grid*, vol.
390 2, no. 1, pp. 198-205, 2011, DOI: 10.1109/TSG.2010.2090913.
- 391 10 M. A. Rostami, A. Kavousi-Fard, and T. Niknam, "Expected Cost Minimization of Smart Grids With Plug-
392 In Hybrid Electric Vehicles Using Optimal Distribution Feeder Reconfiguration," *IEEE Transactions on*
393 *Industrial Informatics*, vol. 11, no. 2, pp. 388-397, 2015, DOI: 10.1109/TII.2015.2395957.
- 394 11 S. Su, H. Li, and D. Gao, "Optimal Planning of Charging for Plug-In Electric Vehicles Focusing on Users'
395 Benefits," *Energies*, vol. 10, no. 7, pp. 952-967, 2017, DOI: 10.3390/en10070952.

- 396 12 P. Olivella-Rosell, R. Villafafila-Robles, A. Sumper, and J. Bergas-Jané, "Probabilistic Agent-Based Model
397 of Electric Vehicle Charging Demand to Analyse the Impact on Distribution Networks," *Energies*, vol. 8,
398 no. 5, pp. 4160-4187, 2015, DOI: 10.3390/en8054160.
- 399 13 M. Schimpe, C. Piesch, H. Hesse, J. Paß, S. Ritter, and A. Jossen, "Power Flow Distribution Strategy for
400 Improved Power Electronics Energy Efficiency in Battery Storage Systems: Development and
401 Implementation in a Utility-Scale System," *Energies*, vol. 11, no. 3, pp. 533-550, 2018, DOI:
402 10.3390/en11030533.
- 403 14 A. Ul-Haq, M. Azhar, Y. Mahmoud, A. Perwaiz, and E. Al-Ammar, "Probabilistic Modeling of Electric
404 Vehicle Charging Pattern Associated with Residential Load for Voltage Unbalance Assessment,"
405 *Energies*, vol. 10, no. 9, pp. 1351-1369, 2017, DOI: 10.3390/en10091351.
- 406 15 H. Bai, S. Miao, P. Zhang, and Z. Bai, "Reliability Evaluation of a Distribution Network with Microgrid
407 Based on a Combined Power Generation System," *Energies*, vol. 8, no. 2, pp. 1216-1241, 2015, DOI:
408 10.3390/en8021216.
- 409 16 A. Ali and D. Söffker, "Towards Optimal Power Management of Hybrid Electric Vehicles in Real-Time:
410 A Review on Methods, Challenges, and State-Of-The-Art Solutions," *Energies*, vol. 11, no. 3, pp. 476-490,
411 2018, DOI: 10.3390/en11030476.
- 412 17 C. Rottondi, S. Fontana, and G. Verticale, "Enabling Privacy in Vehicle-to-Grid Interactions for Battery
413 Recharging," *Energies*, vol. 7, no. 5, pp. 2780-2798, 2014, DOI: 10.3390/en7052780.
- 414 18 C. Cao, L. Wang, and B. Chen, "Mitigation of the Impact of High Plug-in Electric Vehicle Penetration on
415 Residential Distribution Grid Using Smart Charging Strategies," *Energies*, vol. 9, no. 12, pp. 1024-1043,
416 2016, DOI: 10.3390/en9121024.
- 417 19 O. Erdinc, N. G. Paterakis, T. D. P. Mendes, A. G. Bakirtzis, and J. P. S. Catalão, "Smart Household Operation
418 Considering Bi-Directional EV and ESS Utilization by Real-Time Pricing-Based DR," *IEEE Transactions*
419 *on Smart Grid*, vol. 6, no. 3, pp. 1281-1291, 2015, DOI: 10.1109/TSG.2014.2352650.
- 420 20 B. G. Kim, S. Ren, M. v. d. Schaar, and J. W. Lee, "Bidirectional Energy Trading and Residential Load
421 Scheduling with Electric Vehicles in the Smart Grid," *IEEE Journal on Selected Areas in Communications*,
422 vol. 31, no. 7, pp. 1219-1234, 2013, DOI: 10.1109/JSAC.2013.130706.
- 423 21 K. Yuttana, J. Wannawit, B. Krischonme, and M. Nadarajah, "Estimation of the Quick Charging Station
424 for Electric Vehicles based on Location and Population Density Data," *International Journal of Intelligent*
425 *Engineering & Systems*, vol. 11, no. 3, pp. 233-241, June, 2018, DOI: 10.22266/ijies2018.063025.
- 426 22 Maigha and M. Crow, "Economic Scheduling of Residential Plug-In (Hybrid) Electric Vehicle (PHEV)
427 Charging," *Energies*, vol. 7, no. 4, pp. 1876-1898, 2014, DOI: 103990/en7041876.
- 428 23 S.-G. Yoon and S.-G. Kang, "Economic Microgrid Planning Algorithm with Electric Vehicle Charging
429 Demands," *Energies*, vol. 10, no. 10, pp. 1487-1503, 2017, DOI: 10.3390/en10101487.
- 430 24 T. Ma and O. A. Mohammed, "Economic Analysis of Real-Time Large-Scale PEVs Network Power Flow
431 Control Algorithm With the Consideration of V2G Services," *IEEE Transactions on Industry Applications*,
432 vol. 50, no. 6, pp. 4272-4280, 2014, DOI: 10.1109/TIA.2014.2346699.
- 433 25 B. Gao, W. Zhang, Y. Tang, M. Hu, M. Zhu, and H. Zhan, "Game-Theoretic Energy Management for
434 Residential Users with Dischargeable Plug-in Electric Vehicles," *Energies*, vol. 7, no. 11, p. 7499, 2014, DOI:
435 10.3390/en7117499.
- 436 26 H. Liu, Y. Ji, H. Zhuang, and H. Wu, "Multi-Objective Dynamic Economic Dispatch of Microgrid Systems
437 Including Vehicle-to-Grid," *Energies*, vol. 8, no. 5, p. 4476, 2015, DOI: 10.3390/en8054476.

- 438 27 U. Khaled, A. M. Eltamaly, and A. Beroual, "Optimal Power Flow Using Particle Swarm Optimization of
439 Renewable Hybrid Distributed Generation," *Energies*, vol. 10, no. 7, p. 1013, 2017, DOI: 10.3390/en10071013.
- 440 28 P. Kundur, "Power System Stability and Control " *McGraw-Hill: New York*, to be published pp. 272-273,
441 1994.
- 442 29 J. R. Shin, B. S. Kim, M. S. Chae, and S. A. Sebo, "Improvement of precise PV curve considering effects of
443 voltage-dependent load models and transmission losses for voltage stability analysis," *IEEE Proceedings -
444 Generation, Transmission and Distribution*, vol. 149, no. 4, pp. 384-388, 2002, DOI: 10.1049/ip-gtd.20020258.
- 445 30 J. R. Martí, H. Ahmadi, and L. Bashualdo, "Linear Power-Flow Formulation Based on a Voltage-
446 Dependent Load Model," *IEEE Transactions on Power Delivery*, vol. 28, no. 3, pp. 1682-1690, 2013, DOI:
447 10.1109/TPWRD.2013.2247068.
- 448 31 L. M. Hajagos and B. Danai, "Laboratory measurements and models of modern loads and their effect on
449 voltage stability studies," *IEEE Transactions on Power Systems*, vol. 13, no. 2, pp. 584-592, 1998, DOI:
450 10.1109/59.667386.
- 451 32 T. Jen-Hao, "A direct approach for distribution system load flow solutions," *IEEE Transactions on Power
452 Delivery*, vol. 18, no. 3, pp. 882-887, 2003, DOI: 10.1109/TPWRD.2003.813818.
- 453 33 Y. Kongjeen and K. Bhumkittipich, "Modeling of electric vehicle loads for power flow analysis based on
454 PSAT," in *2016 13th International Conference on Electrical Engineering/Electronics, Computer,
455 Telecommunications and Information Technology (ECTI-CON)*, 2016, DOI: 10.1109/ECTICon.2016.7561430, to be
456 published, pp. 1-6, DOI: 10.1109/ECTICon.2016.7561430.
- 457 34 Y. Kongjeen, K. Buayai, and K. Bhumkittipich, "Automate of capacitor placement in microgrid system
458 under EVs load penetration," in *2017 International Electrical Engineering Congress (iEECON)*,
459 2017, DOI: 10.1109/IEECON.2017.8075767, to be published, pp. 1-4, DOI: 10.1109/IEECON.2017.8075767.
- 460 35 R. S. Rao, K. Ravindra, K. Satish, and S. V. L. Narasimham, "Power Loss Minimization in Distribution
461 System Using Network Reconfiguration in the Presence of Distributed Generation," *IEEE Transactions
462 on Power Systems*, vol. 28, no. 1, pp. 317-325, 2013, DOI: 10.1109/TPWRS.2012.2197227.
- 463 36 M. E. Baran and F. F. Wu, "Network reconfiguration in distribution systems for loss reduction and load
464 balancing," *IEEE Transactions on Power Delivery*, vol. 4, no. 2, pp. 1401-1407, 1989, DOI: 10.1109/61.25627.
- 465 37 S. Mishra, D. Das, and S. Paul, "A simple algorithm for distribution system load flow with distributed
466 generation," in *International Conference on Recent Advances and Innovations in Engineering (ICRAIE-2014)*,
467 2014, DOI: 10.1109/ICRAIE.2014.6909127, to be published, pp. 1-5, DOI: 10.1109/ICRAIE.2014.6909127.
- 468